

Mott-Hubbard transition in the mass-imbalanced Hubbard model

Marie-Therese Philipp, Markus Wallerberger, Patrik Gunacker, and Karsten Held
Institute of Solid State Physics, TU Wien, A-1040 Vienna, Austria

The mass-imbalanced Hubbard model represents a continuous evolution from the Hubbard to the Falicov-Kimball model. We employ dynamical mean field theory and study the paramagnetic metal-insulator transition, which has a very different nature for the two limiting models. Our results indicate that the metal-insulator transition rather resembles that of the Hubbard model as soon as a tiny hopping between the more localized fermions is switched on. At low temperatures we observe a first-order metal-insulator transition and a three peak structure. The width of the central peak is the same for the more and less mobile fermions when approaching the phase transition, which agrees with our expectation of a common Kondo temperature and phase transition for the two species.

PACS numbers: 71.27.+a, 71.30.+h

I. INTRODUCTION

Strongly correlated electron systems give rise to a plethora of fascinating physics, and the Mott-Hubbard metal-insulator transition^{1,2} is one of the prime examples. Here, electronic correlations split the non-interacting band so that an insulating state develops, even for an odd number of electrons per site and even without symmetry breaking in the paramagnetic phase. The arguably first satisfactory modeling of this transition was given by Hubbard in the so-called Hubbard-III approximation.³ This is a decoupling of the equation of motion for the Green function based on an alloy analogy, which assumes mobile electrons moving in a lattice of immobile electrons. Physically this solution yields separated Hubbard bands at $\pm U/2$ for large interactions U , and a continuous metal-insulator transition at a critical interaction strength U_c , where both Hubbard bands touch each other, see Fig. 1 (left). Upon further reducing U , the pseudogap gets filled and eventually the non-interacting density of states (DOS) is recovered.⁴ While the Hubbard-III approximation was designed as an approximation for solving the Hubbard model (HM), it already bares the main ingredients of the Falicov-Kimball model (FKM):⁵ mobile and immobile electrons that are coupled through an interaction U . Because of this resemblance, Hubbard³ is sometimes given credit for inventing the FKM.

In particular thanks to insights from dynamical mean field theory (DMFT),^{6,7} we nowadays know that the Mott-Hubbard transition in the Hubbard model is more intricate. First of all, it is first order for temperatures below a critical point, as in the van der Waals liquid-vapor transition. Second, when turning metallic, a quasi-particle resonance develops within the, still pronounced, gap. Consequently a three-peak structure emerges, which only dissolves into a single peak at much smaller interaction strength, see Fig. 1 (right). In contrast, the FKM shows the Hubbard-III type of metal-insulator transition in DMFT^{4,8} as in Fig. 1 (left).

Since these two metal-insulator transitions are genuinely different, we ask in this paper: What is the nature

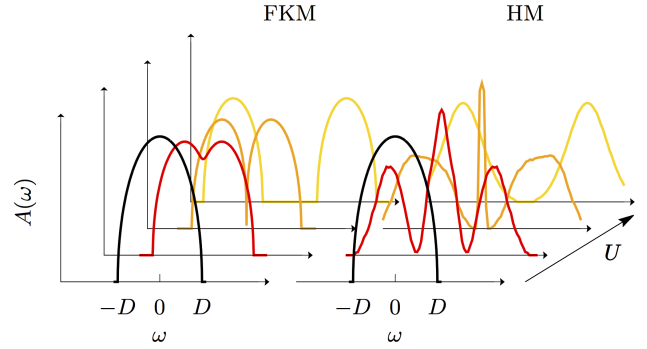


FIG. 1: Schematic view of the Mott-Hubbard metal-insulator transition in the paramagnetic phase of the Falicov-Kimball model (left) and Hubbard model (right). The spectral weight $A(\omega)$ at energy ω is shown along a qualitative interaction-axis U taking into account the shift of the metal-insulator transition.⁹

of the metal-insulator transition when continuously tuning our model from the FKM to the HM?

We address this question by increasing the hopping amplitude of the less mobile fermions from zero (FKM) to the same amplitude as the mobile fermions (HM). As one may construe the different hopping amplitude as a mass difference, one can also perceive this intermediate model as a mass-imbalanced Hubbard model. While the paradigm system for the Mott-Hubbard transition of the HM-type is V_2O_3 ,¹⁰ realizing the mass-imbalanced HM in the solid state is difficult. Usually, there is a Kramers spin-degeneracy and not a strong mass imbalance between the two spin species. However with the advent of cold atom systems, such mass imbalances in a two-component system can be realized readily, either by having different atomic species¹¹ or by generating a spin-dependent hopping through a magnetic field gradient.¹²

On the theoretical side, the antiferromagnetic order in the mass-imbalanced HM has been studied before by DMFT¹³ and quantum Monte Carlo simulation¹⁴, but to the best of our knowledge not the paramagnetic Mott-Hubbard transition which is the topic of the present

paper. Let us mention however that the paramagnetic metal-insulator transition has been addressed quite intensively in the literature for the multi-orbital Hubbard model which has different bandwidths or masses for the two orbitals.^{15–20} Here an orbital-selective Mott transition was found, where first one band and subsequently the second band turns insulating with increasing U . An important and, as we will later see, crucial difference to our situation is however that both orbitals consists of two spin species each.

In the present paper we address the Mott-Hubbard metal-insulator transition in the mass-imbalanced Hubbard model, where both spin species have a different mass or hopping amplitude. This allows us to continuously tune the model from the FKM to the HM. Section II introduces the model and the method employed: DMFT using continuous quantum Monte Carlo simulations as an impurity solver. In Section III we present the calculated phase diagram of the mass-imbalanced HM, the self-energy, spectral function, and double occupancy. In Section IV we discuss the underlying physics of a common Kondo scale for the two fermionic species and support this by numerical data which show that the width of the central quasiparticle peak converges towards the same value for the two different fermions when approaching the metal-insulator transition. Consequently, we observe a single metal-insulator transition and not a spin-dependent one as might be expected from the aforementioned studies on multi-orbital Hubbard model. Finally, Section V summarizes our results.

II. MODEL AND METHOD

The Hamiltonian of the mass-imbalanced Hubbard model for one orbital can be written as:

$$H = -t_c \sum_{\langle ij \rangle} (\hat{c}_i^\dagger \hat{c}_j + \hat{c}_j^\dagger \hat{c}_i) - t_f \sum_{\langle ij \rangle} (\hat{f}_i^\dagger \hat{f}_j + \hat{f}_j^\dagger \hat{f}_i) + U \sum_i \hat{n}_{c,i} \hat{n}_{f,i}, \quad (1)$$

where \hat{c}_i^\dagger (\hat{f}_i^\dagger) and \hat{c}_i (\hat{f}_i) create and annihilate, respectively, one of the two fermion species, while $\hat{n}_{c,i} = \hat{c}_i^\dagger \hat{c}_i$ and $\hat{n}_{f,i} = \hat{f}_i^\dagger \hat{f}_i$ are the corresponding occupancy operators at site i . The hopping between next neighbors, $\langle ij \rangle$, is mediated by the corresponding hopping amplitudes, t_c and t_f ; and it costs the Hubbard interaction U if there is a c and f fermion on the same site i .

In the following, we consider a Bethe lattice, i.e., a semi-elliptic densities of states $D_x(\omega) = \frac{2}{\pi D_x} \sqrt{1 - (\omega/D_x)^2}$ with half bandwidth $D_x \sim t_x$ for the two fermionic species $x = c, f$. In the following, we set $D_c \equiv 2$ as our unit of energy and vary the mass balance²² $D_f/D_c = t_f/t_c$ between 0 and 1.

The two limits of mass imbalance are evident from Eq. (1): In the case $D_f/D_c = 0$, the f fermions are truly frozen and we arrive at the FKM. On the other hand, if

$D_f/D_c = 1$, we can identify c and f with spin-up and spin-down, respectively, and obtain the mass-balanced HM.

The mass-imbalanced HM (1) can be solved exactly using dynamical mean field theory (DMFT), which maps the lattice model self-consistently on a single impurity Anderson model (SIAM).⁷ We use the w2dynamics package,^{23,24} which employs continuous time quantum Monte Carlo (CT-QMC) in the hybridization expansion^{25,26} to solve the auxiliary SIAM. In order to obtain spectral functions $A(\omega)$ in real frequency from the imaginary frequency DMFT Green's function $G(i\omega_n)$, the maximum entropy method (MAXENT) is used.²⁷

Both in the FKM and HM, the metal-insulator transition is shadowed by an anti-ferromagnetic dome for dimension $d \geq 3$. In order to be able to study the Mott transition, we hence enforce the paramagnetic solution and half-filling of both, c and f fermions. In the HM, these constraints can be enforced by explicitly symmetrizing over spins and setting the chemical potential to $\mu = U/2$, respectively. Away from this HM limit, we again enforce half-filling by fixing $\mu = U/2$ such that the total number of fermions per site is $n = 1$. However to ensure the paramagnetic solution at half-filling for both, c and f , fermions individually, we symmetrize the hybridization functions in imaginary time: $\Delta(\tau) \stackrel{\dagger}{=} \Delta(\beta - \tau)$.

III. RESULTS

As mentioned in Section I, the physics of the Mott-Hubbard metal-insulator transition is of first order in the HM ($D_f/D_c = 1$), and hence accompanied by a hysteresis loop in the phase diagram. This hysteresis loop is obtained numerically as follows: Increasing U by taking a DMFT solution of a smaller U as a starting point for the next DMFT iteration, yields a metallic solution up to a critical interaction U_{c1} . Above U_{c1} , the metallic (M) solution is no longer stable and the system becomes Mott-insulating (I) instead. Decreasing U from here, yields an insulating solution down to a second critical interaction $U_{c2} < U_{c1}$. Hence, in the limit of the HM, where c and f fermions are equally mobile, there is a coexistence region of the metallic and the insulating phase for $U_{c2} < U < U_{c1}$. The Mott-Hubbard metal-insulator transition in the HM has been investigated thoroughly in the literature, among others for the semi-elliptic Bethe DOS.^{7,21} In the FKM on the other hand no coexistence region is observed. The Mott-like metal-insulator transition occurs temperature-independent exactly at $U_c = D_c$ in the FKM, as is analytically known and well reviewed in Ref. 8, also see Fig. 1.

Fig. 2 shows the phase diagram D_f/D_c vs. U of the mass-imbalanced HM inbetween these two known limits at two inverse temperatures $\beta = 50$ and 100. The first order coexistence region has been determined in the same way as described above for the HM: The four green sym-

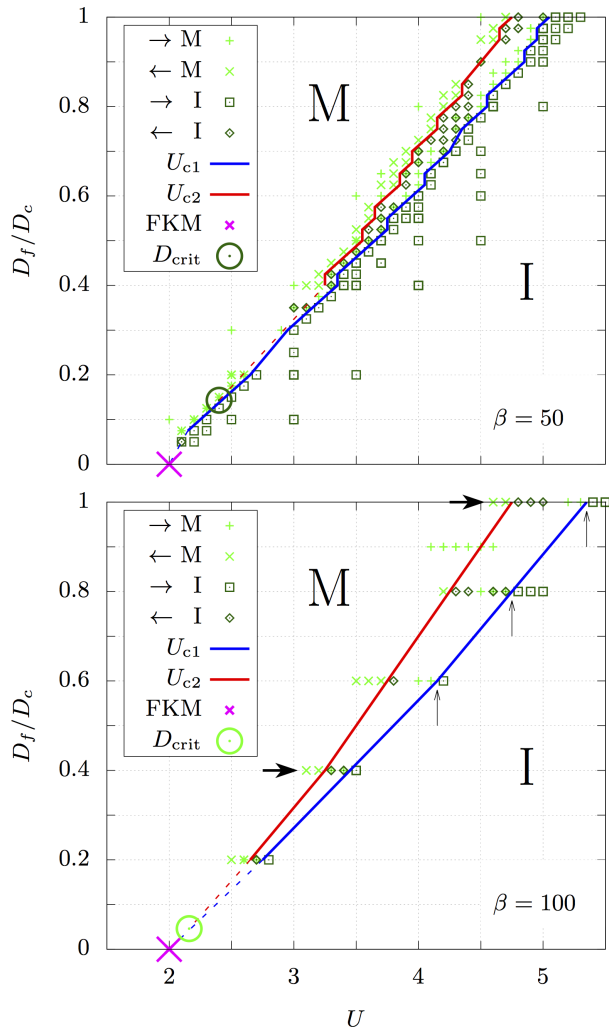


FIG. 2: Phase diagram of the mass-imbalanced Hubbard model as a function of interaction strength U and mass imbalance D_f/D_c at $\beta = 50$ (upper panel) and $\beta = 100$ (lower panel); $D_c \equiv 2$ sets our unit of energy. The critical interaction strengths U_{c1} (blue line) has been obtained by increasing U (\rightarrow) and identifying up to which U value the metallic solution (M, green plus) is still stable and from which U value on we get an insulating solution (I, green boxes). For decreasing U (\leftarrow), U_{c2} (red line) marks the point where the insulating solution (green diamonds) turns metallic (green crosses). The critical point where the first order transition with coexistence region ends is extrapolated by hands of Fig. 4 and indicated here by a green circle. The pink cross denotes the analytical continuous phase transition for the FKM.

bols in Fig. 2 mark up to which point a metallic (M) or insulating (I) solution is found upon increasing or decreasing U . We observe a coexistence region and hence a first order transition in a wide range of mass imbalances. The coexistence region is increasing upon decreasing temperature to $\beta = 100$, and the critical point where the first order transition ends (green circle, D_{crit}) is moving to-

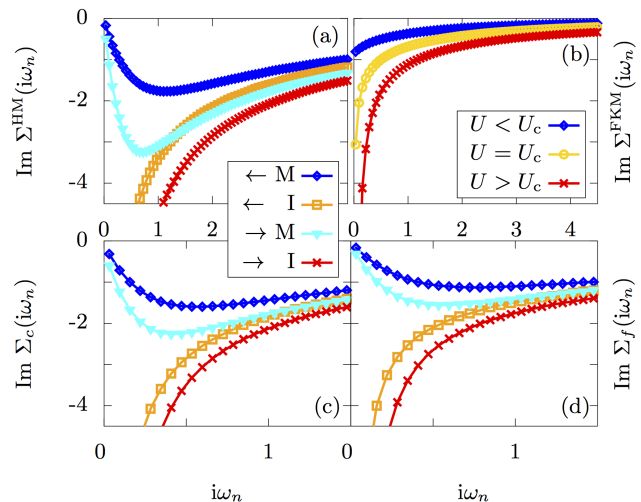


FIG. 3: Imaginary part of the self-energy at $\beta = 100$ as an indicator for a metallic and insulating solution. (a) HM with $D_f/D_c = 1$. (b) FKM with $D_f/D_c = 0$. Lower panel: Comparison of the c fermions (c) and f fermions (d) at the same mass imbalance $D_f/D_c = 0.4$ in a smaller frequency range. Panels (a), (c) and (d) show two metallic (insulating) solutions, one in the purely metallic (insulating) phase (blue (red)) and one within the coexistence region (cyan (orange)). The precise U values of these points are given in the text.

wards the FKM limit $D_f/D_c = 0$. To obtain the phase diagram, we discriminate between metallic and insulating solution by means of the imaginary part of the self-energy $\Sigma(i\omega_n)$.

Fig. 3 shows this imaginary part of the self-energy for exemplary U values at $\beta = 100$. In panel (a) the results for the HM are shown: Specifically, one metallic (M, $U = 4.6$, blue) and one insulating solution (I, $U = 4.9$, orange) upon decreasing U (\leftarrow), as well as one M ($U = 5.2$, cyan) and I solution ($U = 5.5$, red) upon increasing U (\rightarrow). The insulating solution is characterized by a divergence $\Sigma(i\omega_n) \rightarrow -\infty$ for $\omega_n \rightarrow 0$, and we take this as the criterion for discriminating M and I solutions in the phase diagram (Fig. 2).

Fig. 3 (b) displays the results for the FKM: Analogously, one metallic solution ($U = 1.5 < U_c$, blue) and one insulating solution ($U = 2.5 > U_c$, red) are shown. Since there is no coexistence region in the FKM, we instead additionally show the solution for the unique and temperature-independent $U_c = 2$ (yellow).

Fig. 3 (c,d) display analogous phase points though now for the mass-imbalanced HM at a mass imbalance $D_f/D_c = 0.4$, which is inbetween the the limiting cases of the HM (a) and FKM (b). The more mobile c fermions are shown in Fig. 3 (c), and the less mobile f fermions in (d). The shift of the Mott-insulator transition compared to the HM is taken into account by adjusting the interaction strength to $U = 3.2$ (\leftarrow M, blue), $U = 3.3$ (\leftarrow I, orange), $U = 3.4$ (\rightarrow M, cyan) and $U = 3.5$ (\rightarrow I, red) in the two lower panels. We observe that the c fermions

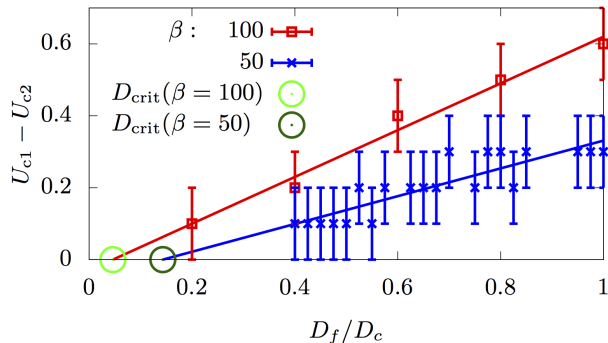


FIG. 4: Difference of the critical interaction strengths, $U_{c1} - U_{c2}$, of the coexistence region vs. the mass imbalance D_f/D_c . The linear extrapolation yields the temperature-dependent critical point D_{crit} at which the first order transition with coexistence region ends.

undergo a stronger renormalization than the already less mobile, and thus heavier, f fermions. That is, in the metallic phase the effective mass enhancement

$$m^*/m = Z^{-1} = 1 - \partial \text{Im}\Sigma(i\omega_n)/\partial i\omega_n|_{i\omega_n \rightarrow 0} \quad (2)$$

is stronger for the c fermions. Nonetheless, the divergent $\text{Im}\Sigma(i\omega_n) \sim -1/(i\omega_n)$ behavior of the self-energy which indicates the insulating phase sets in at the same U value. Overall both self-energies in (c,d) look similar as for the HM in (a) except for the smaller $i\omega_n$ (x -axis) scale, which can be understood from the lower U value of the Mott transition.

In Fig. 4, we extrapolate the coexistence region which is shrinking with decreasing D_f/D_c to $U_{c1} - U_{c2} = 0$. This marks the temperature-dependent critical point $D_{crit}(\beta)$ at which the first order transition ends, denoted by a green circle in Fig. 4. At the lower temperature ($\beta = 100$) this critical point is already very close to the FKM limit $D_f/D_c = 0$, which together with the apparent temperature dependence suggests that indeed for zero temperature $D_{crit}(\beta = \infty) = 0$. In other words, the FKM appears to be the critical point of the mass-imbalanced HM at zero temperature.

The double occupancy in Fig. 5 likewise shows the first order transition and hysteresis loop in U . In the Mott-insulating phase each site is essentially singly occupied. In contrast to when approaching the metallic phase upon decreasing U , the higher kinetic energy leads to a strong increase in the number of doubly occupied sites. Only in the limit $U \rightarrow 0$ the uncorrelated double occupation $\langle \hat{n}_c \hat{n}_f \rangle = 1/4$ is eventually recovered. The figure shows again clearly that the coexistence region increases upon decreasing temperature (increasing β). On that ground the behavior of the mass-imbalanced HM is similar to the HM also regarding the double occupation.

Fig. 6 shows the corresponding spectral function comparing the HM ($D_f/D_c = 1$) and the mass imbalanced

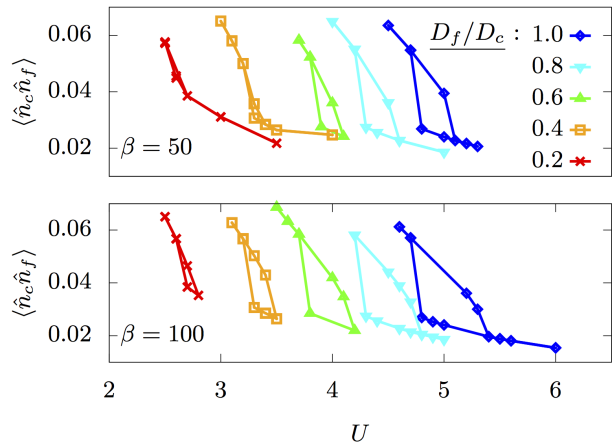


FIG. 5: Double occupancy $\langle \hat{n}_c \hat{n}_f \rangle$ for different values of the mass imbalance D_f/D_c at $\beta = 50$ (upper panel) and $\beta = 100$ (lower panel), showing the hysteresis loop of the first order transition upon increasing and decreasing U .

HM ($D_f/D_c = 0.8$ and 0.6), immediately before (a,c) and after (b,d) the transition U_{c1} where the metallic solution ceases to exist. We see that the spectral functions are actually quite similar with a three-peak structure on the metallic side, consisting of a lower and upper Hubbard band and a central quasiparticle peak inbetween. Immediately after the transition U_{c1} there is a gap in the insulating phase. This is very different from the FKM in Fig. 1 where we have two peaks which do (do not) not overlap any more for U below (above) the transition. There is also no indication of a smooth crossover in Fig. 6 from the HM behavior to that of the FKM. The major difference is that with reducing D_f/D_c in Fig. 6, the position of the upper (lower) Hubbard band shift to higher (lower) energies, which is in agreement with the reduced U_{c1} value at which the transition occurs.

IV. DISCUSSION

The physics in Fig. 6 of the mass-imbalanced HM seems to resemble that of the HM rather than that of the FKM. Also in Fig. 4 we have seen that the first order transition of the HM survives a quite considerable mass imbalance, down to even smaller D_f/D_c values at lower temperatures. We know on the other hand that there is no first order transition for the FKM. This poses the questions whether at zero temperature $D_{crit} = 0$, i.e., there is always a first order transition for $D_f > 0$? Is the FKM and its physics a singular point of the mass-imbalanced Hubbard model at zero temperature? Indeed the temperature dependence in Fig. 4 already suggests $D_{crit} = 0$.

Let us further address this question by considering the underlying DMFT impurity problem which will help us to identify the fundamental physics. In the case of the

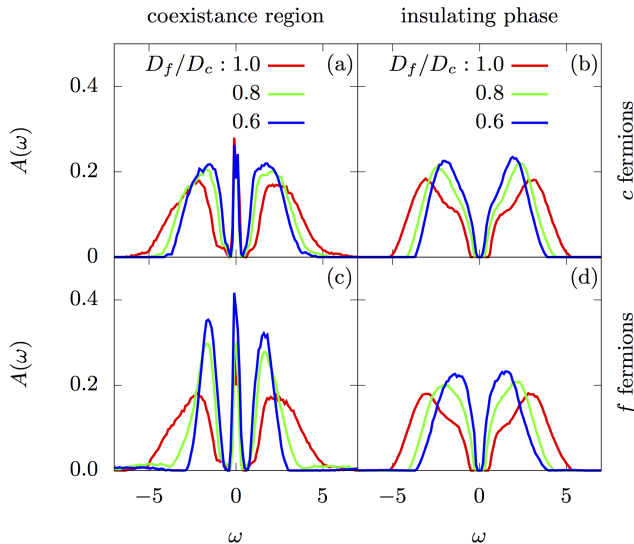


FIG. 6: Spectral function $A(\omega)$ near the critical interaction strength U_{c1} for different mass imbalances D_f/D_c at $\beta = 100$. The upper and lower two panels show the more and less mobile c and f fermions, respectively. The left (right) panels show a metallic (insulating) solution just below (above) U_{c1} , indicated by the three vertical arrows in Fig. 2. Specifically the D_f, U values for the left panels (a) and (c) are: $D_f = 2.0$, $U = 5.2$ (red); $D_f = 1.6$, $U = 4.1$ (green); $D_f = 1.2$, $U = 3.4$ (blue); and for the right panels (b) and (d): $D_f = 2.0$, $U = 5.5$ (red); $D_f = 1.6$, $U = 4.2$ (green), $D_f = 1.2$, $U = 3.5$ (blue).

HM, DMFT corresponds to the self-consistent solution of the Anderson impurity model,⁷ whereas for the FKM one needs to iterate the resonant level model.⁸ In case of the mass-imbalanced HM, we have an Anderson impurity type of model but with a different bath for the more mobile c and the less mobile f fermions.

Specifically the DMFT impurity problem of the mass-imbalanced HM has, in case of the Bethe lattice, the following non-interacting Green function

$$\mathcal{G}_x^{-1}(\omega) = \omega + \mu - (D_x/2)^2 G_x(\omega) \equiv \omega + \mu - \Delta_x(\omega), \quad (3)$$

given by the interacting Green function $G_x(\omega)$ at frequency ω .⁷ This can be understood as follows: if a fermion leaves the impurity with amplitude $D_x/2$ it propagates through the strongly correlated bath of the other sites given by $G_x(\omega)$ before returning to the impurity with amplitude $D_x/2$. The difference for the mass-imbalanced HM is now that each fermion species $x = c, f$ has an individual bath or hybridization function $\Delta_x(\omega)$.

On the metallic side, close to the metal-insulator transition we have seen a narrow central resonance in Fig. 6, and we can map the Anderson impurity model onto a Kondo model with different baths. For a narrow resonance, we are in the Kondo regime and can apply the perturbative renormalization group also known as Anderson's poor man scaling^{28,29} for understanding the

physics. For the renormalization of the Kondo coupling, the spectral weight at high energies, i.e., in the upper and lower Hubbard band does not matter³⁰ and we can restrict ourselves to the central resonance.³¹

Since the Kondo effect relies on spin-flip (i.e., c - f) scattering,²⁹ it is not possible that the coupling to the bath for one species alone becomes large in the renormalization process whereas the other does not. The two fermionic species make the Kondo effect at essentially the same Kondo temperature and develop a Kondo resonance together. This also implies that the physical origin of the central resonance and its width is the same for c and f fermions in Fig. 6. The height of the central resonance, on the other hand, is independent of D_f for the c fermions (note $D_c = 2$ is fixed), whereas it increases $\sim 1/D_f$ for the less mobile f fermions as does the non-interacting DOS of the f fermions.

We can validate this expectation numerically by estimating the width of the central resonance as $Z_x D_x$, where Z_x is the quasiparticle renormalization as calculated from the self-energy through Eq. (2). If the width $Z_x D_x$ is to be the same for the $x = c, f$ fermions, the quasiparticle renormalization Z_f needs to be larger since $D_f < D_c$. Indeed a first indications for this we have already seen in the smaller f self-energy and hence larger Z_f in Fig. 3.

Fig. 7 shows the analysis of the quasiparticle renormalized width $Z_x D_x$ for the two fermionic species x . Indeed we see that $Z_c D_c \rightarrow Z_f D_f$ as the metal-insulator transition is approached, in agreement with our considerations above. In contrast, at $U = 0$ where $Z_x = 1$ the width is obviously very different. For the exemplary green line in Fig. 7, we see the continuous evolution from a factor of 0.6 difference in width at $U = 0$ to the same width in the Kondo regime in the vicinity of the phase transition line U_{c1} .

The observation that $Z_c D_c \rightarrow Z_f D_f$ for $U \rightarrow U_{c1}$ also implies a simultaneous phase transition for both fermionic species, in agreement with our observation for the self-energy in Fig. 3 and the phase diagram Fig. 2 above. This is in contrast to the multi-orbital HM for which an orbital-selective phase transition has been observed.¹⁵⁻²⁰ The striking difference is that for the multi-orbital HM we have two spin species for each orbital so that the Kondo effect can occur separately for each orbital which is not possible in our case of the mass-imbalanced HM.

Altogether, the physics of the mass-imbalanced HM for $D_f > 0$ rather resembles that of the HM than that of the FKM. Noteworthy, however, one needs ever lower temperatures with decreasing D_f in order for the central resonance to develop since the joint Kondo temperature decreases exponentially. The similar physics to the HM further suggest the same first order metal-insulator transition. Indeed the temperature dependence of the critical point in Fig. 4 already suggested that the transition is of first order for any $D_f > 0$ at zero temperature. Let us note however that while the similar physics sug-

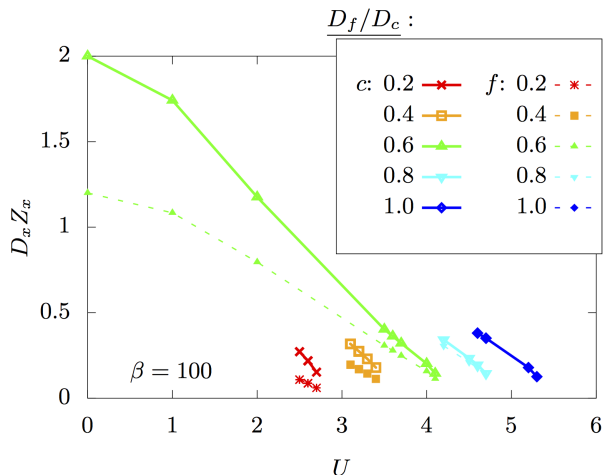


FIG. 7: Width of the central quasiparticle peak $Z_x D_x$ for the fermionic species $x = c, f$ (solid line, dashed line) vs. U at $\beta = 100$ and different values of the mass imbalance D_f/D_c .

gests the same first-order nature of the phase transition, in principal there could also be a continuous transition in the HM given the underlying Kondo physics. Indeed whether the phase transition is of first order in the HM was quite debated in the early days of DMFT³²⁻³⁴ and eventually had to be decided numerically. In our case of the mass-imbalanced HM our numerical data strongly indicates that the phase transition already becomes first order as soon as there is a finite hopping of the f fermions ($D_f > 0$).

V. CONCLUSION

We have analyzed the Mott-insulator transition of the mass-imbalanced Hubbard model within the paramagnetic phase. Our phase diagram, Fig. 2, shows a first order phase transition in a wide range of mass imbalances D_f/D_c . With decreasing temperature the region of first order coexistence expands; and our results suggest that the mass-imbalanced Hubbard model always displays a first order metal-insulator transition at zero temperature as soon as a small, but finite, hopping of the less mobile f fermions is switched on ($D_f > 0$).

For the FKM ($D_f = 0$), we have two bands along with a gap opening with increasing U as soon as these two bands do not overlap any longer. If we switch on f fermion hopping however ($D_f > 0$), a central resonance in this gap develops due to the Kondo effect. This sta-

bilizes the metallic phase and shifts the metal-insulator transition in the phase diagram Fig. 2 towards larger U values. This resonance and a three-peak structure can be seen in the spectral function, Fig. 6. We find that the width of the central resonance is the same for the c and f fermions. This can be understood from the fact that the spin-flip (here c - f) scattering is crucial for the Kondo effect. Hence we have a joint Kondo temperature and width of the Kondo resonance for c and f fermions.

This is affirmed by an analysis of the quasiparticle renormalization factor Z_x in Fig. 7, which shows $Z_c D_c \rightarrow Z_f D_f$ when approaching the metal-insulator transition, i.e. when we are in the Kondo regime accompanied by a narrow central resonance. It further shows that the metal-insulator transition occurs simultaneously for both, c and f , fermions in the mass-imbalanced Hubbard model. The Falicov-Kimball physics, where the f fermions are insulating for any U and the c fermions for $U > D_c$, is a singular point of the phase diagram at zero temperature.

Altogether our results show that the physics of the mass-imbalanced Hubbard model in the paramagnetic phase resembles that of the Hubbard model. This is because of the equalizing power of the joint Kondo effect of the two fermionic species. Regarding the antiferromagnetic phase we nonetheless expect a qualitatively different behavior: the mass imbalance breaks the c - f O(3) rotational symmetry of the order parameter; and Monte-Carlo simulations¹⁴ indeed indicate an Ising-type ordering. Hence we expect Ising-type critical exponents similar to what has recently been reported for the FKM,³⁵ whereas we have a Heisenberg-type of ordering and associated critical exponents³⁶ for the Hubbard model.

VI. ACKNOWLEDGMENT

We thank B. Hartl, C. Taranto, P. Thunström, A. Toschi, T. Ribic, and V. Zlatić for useful discussions, as well as A. Sandvik for making available his maximum entropy program. This work has been supported by European Research Council under the European Union's Seventh Framework Program (FP/2007-2013)/ERC through grant agreement n. 306447; the Vienna Scientific Cluster (VSC) Research Center funded by the Austrian Federal Ministry of Science, Research and Economy (bmfwf); and the Austrian Science Fund (FWF) through SFB Vi-CoM F41 and project I-610-N16 as part of the research unit FOR 1346 of the Deutsche Forschungsgemeinschaft (DFG). Calculations have been done on the Vienna Scientific Cluster (VSC).

¹ F. Gebhard, *The Mott metal-insulator transition* (Springer-Verlag, Berlin, 1997).

² M. Imada, A. Fujimori, Y. Tokura, *Rev. Mod. Phys.* **70**,

1039 (1998).

³ J. Hubbard, *Proc. R. Soc. London, Ser. A* **276**, 238 (1963).

⁴ P. G. J. van Dongen and C. Leinung, *Ann. Phys. (Leipzig)*

- 509**, 45 (1997).
- ⁵ L. M. Falicov and J. C. Kimball, Phys. Rev. Lett. **22**, 997 (1969).
 - ⁶ A. Georges and G. Kotliar, Phys. Rev. B **45** 6479 (1992).
 - ⁷ A. Georges, G. Kotliar, W. Krauth, and M. J. Rozenberg, Rev. Mod. Phys. **68**, 13 (1996).
 - ⁸ J. K. Freericks and V. Zlatić, Rev. Mod. Phys. **75**, 1333 (2003).
 - ⁹ DMFT spectra for the FalicovKimball model have been calculated analytically at $U = 0, 1.5, 2.0, 5.2$; $D = 2$; those of the Hubbard model have been calculated at $U = 0, 4.0, 5.2, 5.5$; $D = 2$ using continuous quantum Monte Carlo simulations as a DMFT impurity solver and the maximum entropy method.
 - ¹⁰ P. Hansmann, A. Toschi, G. Sangiovanni, T. Saha-Dasgupta, S. Lupi, M. Marsi, K. Held, physica status solidi (b) **250**, 1251 (2013).
 - ¹¹ M. Taglieber, A.-C. Voigt, T. Aoki, T. W. Hänsch, and K. Dieckmann, Phys. Rev. Lett. **100**, 010401 (2008).
 - ¹² G. Jotzu, M. Messer, F. Görg, D. Greif, R. Desbuquois, and T. Esslinger, Phys. Rev. Lett. **115**, 073002 (2015).
 - ¹³ A. Sotnikov, D. Cocks, and W. Hofstetter, Phys. Rev. Lett. **109**, 065301 (2012).
 - ¹⁴ Y.-H. Liu and L. Wang, Phys. Rev. B **92**, 235129 (2015).
 - ¹⁵ A. Liebsch, Europhys. Lett. **63** 97 (2003).
 - ¹⁶ A. Koga, N. Kawakami, T. M. Rice and M. Sigrist, Phys. Rev. Lett. **92** 216402 (2004).
 - ¹⁷ S. Biermann, L. de' Medici and A. Georges, Phys. Rev. Lett. **95** 206401 (2005).
 - ¹⁸ R. Arita and K. Held, Phys. Rev. B **72** 201102(R) (2005).
 - ¹⁹ C. Knecht, N. Blümer and P. G. J. van Dongen, Phys. Rev. B **72** 081103 (R) (2005).
 - ²⁰ M. Ferrero, F. Becca, M. Fabrizio and M. Capone, Phys. Rev. B **72** 205126 (2005).
 - ²¹ N. Blümer, PhD thesis, Universität Augsburg (2003)
 - ²² Let us note here that in the literature²⁰ sometimes a mass *imbalance* factor $\zeta \equiv (t_c - t_f)/(t_c + t_f)$ is used instead of our t_f/t_c .
 - ²³ N. Parragh, A. Toschi, K. Held, and G. Sangiovanni, Phys. Rev. B **86** 155158 (2012).
 - ²⁴ M. Wallerberger, PhD thesis, Technische Universität Wien (2016).
 - ²⁵ P. Werner, A. J. Millis, Phys. Rev. B **74**, 155107 (2006).
 - ²⁶ E. Gull, A. J. Millis, A. I. Lichtenstein, A. N. Rubtsov, M. Troyer, and P. Werner, Rev. Mod. Phys. **83**, 349 (2016).
 - ²⁷ M. Jarrell and J. E. Gubernatis, Phys. Rep. **269**, 133 (1996).
 - ²⁸ P. W. Anderson, J. Phys. C: Solid State Phys. **3**, 2436 (1970).
 - ²⁹ A. C. Hewson, *The Kondo Problem to Heavy Fermions*, Cambridge Studies in Magnetism Vol. 2 (Cambridge University Press, Cambridge 1993).
 - ³⁰ At least as long as these Hubbard bands are well enough separated from the central resonance.
 - ³¹ K. Held, R. Peters, A. Toschi, Phys. Rev. Lett. **110**, 246402 (2013).
 - ³² A. Georges and G. Kotliar, Phys. Rev. B **45**, 6479 (1992).
 - ³³ J. Schlipf, M. Jarrell, P. G. J. van Dongen, N. Blümer, S. Kehrein, Th. Pruschke, and D. Vollhardt Phys. Rev. Lett. **82**, 4890 (1999).
 - ³⁴ M. J. Rozenberg, R. Chitra, and G. Kotliar, Phys. Rev. Lett. **83**, 3498 (1999).
 - ³⁵ A. E. Antipov, E. Gull, and S. Kirchner, Phys. Rev. Lett. **112**, 226401 (2014).
 - ³⁶ G. Rohringer, A. Toschi, A. A. Katanin, and K. Held, Phys. Rev. Lett. **107**, 256402 (2011).